

# Overexpression of Interleukin-18 Aggravates Cardiac Fibrosis and Diastolic Dysfunction in Fructose-Fed Rats

Shan-Shan Xing,<sup>1,2</sup> Xiu-Ping Bi,<sup>1,3</sup> Hong-Wei Tan,<sup>1</sup> Yun Zhang,<sup>1</sup> Qi-Chong Xing,<sup>4</sup> and Wei Zhang<sup>1</sup>

<sup>1</sup>Key Laboratory of Cardiovascular Remodeling and Function Research, Chinese Ministry of Education and Chinese Ministry of Public Health, Department of Cardiology, QiLu Hospital, Shandong University, Jinan, China; <sup>2</sup>Shandong University of Traditional Chinese Medicine, Jinan, China; <sup>3</sup>Department of Cardiology, Jinan Central Hospital, affiliated with Shandong University, Jinan, China; <sup>4</sup>Department of Cardiology, Shandong Provincial Qianfoshan Hospital, Shandong University, Jinan, China

Inflammation plays an important role in the pathophysiology of the metabolic syndrome (MS). We determined whether the overexpression of interleukin (IL)-18 could aggravate left ventricular (LV) remodeling and diastolic dysfunction in fructose-fed rats (FFRs). To create an animal model for MS, male Wistar rats received 10% fructose in water for 8 months. We used an adenovirus encoding rat IL-18 to overexpress IL-18 in FFRs by intravenous administration. IL-18 overexpression led to increases in collagen volume fraction and collagen deposition. LV systolic function was unaltered. But the LV end-diastolic pressure and the time constant of isovolumic relaxation ( $\tau$ ) were increased. Peak negative value of time derivative of LV pressure ( $-dp/dt$ ) was decreased. Isovolumic relaxation time and myocardial index, as assessed by echocardiography, were increased. Overexpression of IL-18 leads to aggravated LV remodeling and dysfunction in FFRs. Attenuation of the inflammatory process may provide a novel therapeutic strategy in treating metabolic cardiomyopathy.

© 2010 The Feinstein Institute for Medical Research, [www.feinsteininstitute.org](http://www.feinsteininstitute.org)

Online address: <http://www.molmed.org>

doi: 10.2119/molmed.2010.00028

## INTRODUCTION

Presence of obesity, non-insulin-dependent diabetes mellitus and hypertension is an essential feature of the metabolic syndrome (MS), which is associated with the development and progression of cardiovascular disease (1). Recently, population-based studies report that MS patients also present mild but significant left ventricular (LV) diastolic dysfunction (2,3). Cardiac fibrosis, a major cause of diastolic dysfunction, is prevalent in these MS patients. Collagen type I and collagen type III are the major fibrillar collagens present in the adult heart. Excessive interstitial collagens in the myocardium are associated with organ stiffness and result in dia-

stolic dysfunction leading to heart failure.

Clinical studies demonstrate that serum interleukin (IL)-18 is elevated in patients with MS, and IL-18 levels are associated with MS independent of obesity and insulin resistance, suggesting that activation of IL-18 is involved in the pathogenesis of MS (4). IL-18 experimentally has been shown to induce production of tumor necrosis factor- $\alpha$  (5), IL-1 $\beta$  (5), IL-6 (6) and inducible nitric oxide synthase (6), which have all been associated with myocardial dysfunction (7–9). To date, however, the effect of IL-18 on MS remains obscure.

Recent studies have shown that daily administration of IL-18 in healthy mice

induces LV dysfunction and blunts  $\beta$ -adrenergic responsiveness to isoproterenol (10). Moreover, induction of myocardial hypertrophy by IL-18 indicates a role for this cytokine in myocardial remodeling. Our group has previously shown (11) that perivascular fibrosis around coronary arterioles is evident in fructose-fed rats (FFRs), which was accompanied by a parallel increase in IL-18, as demonstrated by immunohistochemical analysis and real-time polymerase chain reaction. It is unclear, however, whether IL-18 upregulation may cause function alterations during MS. In the current study, we investigated the functional consequences of IL-18 overexpression in the FFRs.

## MATERIALS AND METHODS

### Preparation of Adenovirus Carrying the IL-18 Gene

Adenovirus containing the IL-18 gene (Ad-IL-18) and the control virus containing the GFP gene (Ad-GFP) were generously provided by the Key Laboratory of Cardiovascular Remodeling and Func-

---

**Address correspondence and reprint requests to** Qi-Chong Xing, Department of Cardiology, Shandong Provincial Qianfoshan Hospital, Shandong University, 66 Jingshi Road, Jinan 250014, China. Phone: 0086-531-82963056; Fax: 0086-531-86169356; E-mail: [xingqichong@163.com](mailto:xingqichong@163.com); or Wei Zhang, Department of Cardiology, Shandong University QiLu Hospital, 250012, 107 West Wenhua Road, Jinan, China. Phone: 0086-531-82963056; Fax: 0086-531-86169356; E-mail: [professor-zhangwei@163.com](mailto:professor-zhangwei@163.com).

Submitted February 27, 2010; accepted for publication July 9, 2010; Epub ([www.molmed.org](http://www.molmed.org)) ahead of print July 12, 2010.

tion Research (QiLu Hospital, Shandong University, Jinan, China). These adenoviruses have been used in previous studies (12).

### Animals and Experimental Treatments

All rats were handled in accordance with the Animal Management Rules of the Ministry of Health, People's Republic of China (documentation 55, 2001), and experimental protocol was approved by the Institutional Animal Care Committee of Shandong University. Six-week-old male Wistar-Kyoto rats, purchased from the Animal Research Institution of Shandong University School of Medicine, were housed in individual cages at room temperature, with a 12-h light–12-h dark cycle (7 am to 7 pm). Rats were randomly assigned to two groups: control ( $n = 12$ ) and fructose ( $n = 31$ ) groups. Rats in the fructose group were given 10% fructose in drinking water and standard chow (16% protein, 8% fat, 50% carbohydrate, 22% trace elements) *ad libitum*, whereas rats in the control group had free access to tap water and standard chow. After being fed for 8 months, the rats of the fructose group were randomly divided into three groups: the fructose group ( $n = 9$ ), MS-GFP group ( $n = 9$ ) and MS-IL-18 group ( $n = 13$ ). The rats in MS-IL-18 and MS-GFP groups were injected through the tail vein with  $1 \times 10^{10}$  plaque-forming units of adenovirus harboring *IL-18* (MS-IL-18 group) or *GFP* gene (MS-GFP group), respectively. The control and fructose groups received an equal volume of drug-free vehicle (normal saline solution). At 6 weeks, the echocardiographic parameters and the hemodynamic parameters were analyzed, and the animals were then euthanized. Tissues were harvested for morphological and biochemical analyses.

### Echocardiographic Studies

Rats were anesthetized with 1.5–2.0% isoflurane by mask, with the chest shaved, and then situated in the supine position on a warming pad. Two-dimensionally guided M-mode recordings were obtained from the long-axis view by using a

GE Vivid 7 system with a GE S10-MHz phased-array transducer (General Electric). Measurements of LV end-diastolic diameter (LVEDD), LV end-systolic diameter (LVESD), septum diastolic wall thickness (SWd) and posterior diastolic wall thickness (PWd) were made according to American Society of Echocardiography guidelines (13). Ejection fraction (EF) was calculated as  $EF = (LVEDD^3 - LVESD^3) / LVEDD^3 \times 100\%$  and shortening fraction (SF) was calculated as  $SF = (LVEDD - LVESD) / LVEDD \times 100\%$ .

Mitral flow was recorded at the tip of the mitral valve from an apical four-chamber view using pulsed Doppler. Because the heart rate was  $>300$  beats/min in most rats, it was difficult to clearly identify the *A* wave on transmitral flow velocity spectra. For this reason, measurement of the peak velocity of the *A* wave and DT was much less feasible than *E* wave measurement in all four groups. From the five-chamber apical view, aortic flow was recorded using pulsed Doppler with the smallest sample volume (0.06 cm) placed at the level of the aortic annulus. LV ejection time (ET) was measured from the beginning to the end of the aortic flow wave. The isovolumic relaxation time was measured as the interval between aortic closure and the start of mitral flow. Using the same tracing, we measured the time between the closing and opening of the aortic valve (DD) and between the opening and closing of the mitral valve (MD). The myocardial index (MI) described by Tei *et al.* (14) was calculated as follows:  $MI = (DD - MD) / ET$ .

Using pulsed Doppler tissue imaging, we also recorded early lateral mitral annulus movement (*Ea*) from the apical view as previously described (15). All measured and calculated indexes are presented as the average of three to five consecutive measurements.

### In Vivo Hemodynamic Measurements

Rats were intubated, ventilated and anesthetized (1.5–2.0% isoflurane). A 3.5-Fr microtipped pressure transducer (Millar Instruments, Houston,

TX, USA) was introduced into the LV via the right carotid artery. Heart rate, LV systolic pressure (LVSP), LV end-diastolic pressure (LVEDP), peak positive value of time derivative of LV pressure ( $+dp/dt$ ) and  $-dp/dt$  were recorded simultaneously using a data acquisition system (RM6000, Nihon Kohden Corporation, Shinjuku-ku, Japan), and *tau* was calculated automatically from LV tracings. Because  $-dp/dt$  was demonstrated to be related and dependent on LVSP (14), we divided  $-dp/dt$  by LVSP [ $(-dp/dt) / LVSP$ ]. The measurement was done in 10 consecutive cardiac cycles, and values were then averaged.

### Total Collagen Staining and Morphometric Measurement

Rats were killed immediately after the hemodynamic study. The heart was rapidly excised and immersed in ice-cold buffer. The left ventricle was separated from the right ventricle, the atria and the great vessels. A portion of the left ventricle was harvested for histopathology, and the remaining was frozen in liquid nitrogen and stored at  $-80^\circ\text{C}$ .

LV specimens fixed in 4% paraformaldehyde were embedded in paraffin and cut into 5- $\mu\text{m}$ -thick sections. The sections were then deparaffinized in xylene, dehydrated with graded concentrations of alcohol and stained with Masson's Trichrome stain (16). For each image, collagen volume fraction was determined as the ratio of collagen surface area stained with aniline blue with respect to myocardial surface area.

Morphometric measurements were conducted by systematically scanning the regions using a light microscope (BX-51, Olympus, Japan) at a magnification of 400 $\times$  by an investigator blinded to the groups. Fields containing vessels, artifacts or incomplete tissue were excluded. Each image was analyzed using hue, saturation and intensity detection modes of the Leica Qwin Image Analyzer (Leica, London, UK) under standardized brightness and contrast according to the user manual of the software. Mean values of at least 15 fields were taken in each region of the heart for subsequent experiments.

## Immunohistochemistry

Serial cryostat transverse sections of 5  $\mu\text{m}$  thickness were fixed in acetone for 10 min, air-dried and stained by the indirect immunohistologic method. Tissue sections were treated with 0.3%  $\text{H}_2\text{O}_2$  solution for 10 min to inhibit endogenous peroxidase activity and were then incubated with blocking solution (5% cow serum; Santa Cruz Biotechnology, Santa Cruz, CA, USA) for 20 min. To evaluate myocardial collagen type I and III levels, mouse monoclonal antibodies to collagen type I and III (Abcam, Cambridge, UK) at a 1:500 dilution were used. After being washed in phosphate-buffered saline for 10 min, the sections were incubated with secondary goat anti-mouse antibody and visualized with 3-amino-9-ethyl carbazole (Santa Cruz Biotechnology) as substrate. The nuclei were counterstained with hematoxylin, and the sections were viewed with a light microscope at a magnification of  $\times 400$ .

## RNA Extraction and Real-Time RT-PCR

Total RNA was extracted from left ventricles using TRIzol reagents (Invitrogen, Carlsbad, CA, USA) according to the manufacturer's protocol. After DNase (RQ1; Promega, Madison, WI, USA) treatment, 1  $\mu\text{g}$  total RNA was reverse-transcribed using random primers and Moloney murine leukemia virus (M-MLV) reverse transcriptase (Promega). A 2- $\mu\text{L}$  aliquot of the cDNA was amplified by real-time PCR in 20  $\mu\text{L}$  PCR mixture using SYBR Green Master Mix with the Light Cycler 2.0 (LCS4 4.0.0.23; Roche, Basel, Switzerland). The primer sequences were as follows: type I collagen (forward 5'-GGA GAG TAC TGG ATC GAC CCT AAC-3'; reverse 5'-CTG ACC TGT CTC CAT GTT GCA-3'), type III collagen (forward 5'-GAA AAA ACC CTG CTC GGA ATT-3'; reverse 5'-GGA TCA ACC CAG TAT TCT CCA CTC T-3'). Expression levels were normalized to the reference gene *GADPH* (forward 5'-TGC CAA GTA TGA TGA CAT CAA GAA G-3'; reverse 5'-AGC CCA GGA TGC CCT TTA GT-3'). At the end of each PCR run, the data were automatically analyzed by the system, and amplification

**Table 1.** Echocardiographic data.

	Control group (n = 12)	Fructose group (n = 9)	MS-GFP group (n = 9)	MS-IL-18 group (n = 13)
LVEDD (mm)	5.93 $\pm$ 0.51	6.68 $\pm$ 0.47**	6.60 $\pm$ 0.48**	6.59 $\pm$ 0.59**
SWd (mm)	1.17 $\pm$ 0.16	1.44 $\pm$ 0.14*	1.38 $\pm$ 0.13*	1.49 $\pm$ 0.36**
PWd (mm)	1.16 $\pm$ 0.19	1.34 $\pm$ 0.13*	1.33 $\pm$ 0.19*	1.44 $\pm$ 0.22**
E (m/s)	111.4 $\pm$ 10.2	94.9 $\pm$ 7.6**	95.0 $\pm$ 10.3**	88.3 $\pm$ 5.6**
Ea (cm/s)	7.1 $\pm$ 1.2	5.4 $\pm$ 1.2**	5.4 $\pm$ 1.5**	4.9 $\pm$ 1.2**
E/Ea	16.2 $\pm$ 3.2	18.2 $\pm$ 4.0	19.0 $\pm$ 6.9	19.6 $\pm$ 6.4
Isovolumic relaxation time (ms)	11.09 $\pm$ 1.37	12.94 $\pm$ 1.53**	12.93 $\pm$ 1.44**	14.79 $\pm$ 1.85***§§
Myocardial index	0.33 $\pm$ 0.04	0.43 $\pm$ 0.03**	0.43 $\pm$ 0.03**	0.47 $\pm$ 0.04***§§
Ejection fraction (%)	81.8 $\pm$ 4.1	83.1 $\pm$ 4.6	83.4 $\pm$ 5.1	82.9 $\pm$ 5.2
Shortening fraction (%)	47.2 $\pm$ 3.3	48.4 $\pm$ 2.4	47.6 $\pm$ 3.1	48.1 $\pm$ 2.8

Data are expressed as means  $\pm$  SD. E, peak velocity of early mitral inflow; Ea, early diastolic velocity of the mitral annulus; \* $P$  < 0.05, \*\* $P$  < 0.01 versus the control group; \*\*\* $P$  < 0.01 versus the fructose group; §§ $P$  < 0.01 versus the MS-GFP group.

plots were obtained. Melting curve analysis was performed to assess the specificity of the PCR products. All amplification reactions were performed in triplicate.

## Statistical Analysis

Data are expressed as mean  $\pm$  SD. All continuous variables were normally distributed before analyzed by ANOVA. Furthermore, we used the Bartlett test to analyze the homoscedasticity of the variables. A probability of  $P$  < 0.05 was considered statistically significant. SPSS version 13.0 for Windows was used for the analysis.

## RESULTS

### Echocardiographic Studies

Echocardiography was successful in every case. Compared with the controls, the hearts of FFRs showed structural changes such as increased LVEDD, SWd, and PWd (Table 1). Functional abnormalities accompanied structural remodeling of the LV. The E wave and the Ea wave were significantly lower, and isovolumic relaxation time was significantly elevated in FFRs. These changes indicate that there is a modest decline in LV diastolic function in FFRs. As shown in Table 1, isovolumic relaxation time and myocardial index were significantly elevated in the IL-18-overexpressing rats compared with the Ad-GFP-infected rats. This suggests that overexpression of IL-18 aggra-

vates diastolic dysfunction in FFRs. SWd and PWd tended to be higher in MS-IL-18 rats than in FFRs, which did not reach statistical significance ( $P$  = 0.072). Systolic function, as assessed by ejection fraction and shortening fraction, was not significantly different among four groups of rats.

### In Vivo Hemodynamics

The hemodynamic measurements could not be performed in three control rats, two FFRs, two MS-GFP rats and four MS-IL-18 rats because of technical difficulties. Heart rate and  $+\text{dp}/\text{dt}$  were similar during an invasive hemodynamic study (Table 2). As expected in this model, LVSP, LVEDP and  $\tau$  were significantly increased, and  $-\text{dp}/\text{dt}$  was decreased in FFRs. The load-independent index of relaxation, namely,  $-\text{dp}/\text{dt}/\text{LVSP}$ , was significantly lower in FFRs, demonstrating a slower relaxation rate in FFRs. Overexpression of IL-18 did not change the systolic parameters, but significantly altered the diastolic parameters, as evidenced by decreases in  $-\text{dp}/\text{dt}$  and  $-\text{dp}/\text{dt}/\text{LVSP}$  and increases in LVEDP and  $\tau$ .

### Collagen Volume Fraction

Histological and morphometric analyses showed that the degree of cardiac fibrosis, expressed as collagen volume fraction, was increased ( $6.72 \pm 1.97$  ver-

**Table 2.** *In vivo* hemodynamic data.

	Control group (n = 9)	Fructose group (n = 7)	MS-GFP group (n = 7)	MS-IL-18 group (n = 9)
Heart rate (beat/min)	380 ± 15	378 ± 14	378 ± 12	380 ± 14
LVSP (mmHg)	117.3 ± 10.2	158.4 ± 14.2**	158.3 ± 9.5**	165.3 ± 9.1**
LVEDP (mmHg)	6.4 ± 1.5	15.1 ± 1.6**	15.2 ± 1.1**	17.8 ± 1.1**##§§
+dp/dt (mmHg/s)	5,463 ± 223	5,454 ± 206	5,461 ± 213	5,455 ± 202
-dp/dt (mmHg/s)	5,045 ± 194	4,889 ± 99*	4,887 ± 125*	4,766 ± 79**##§
(-dp/dt)/LVSP (s <sup>-1</sup> )	43 ± 5	31 ± 3**	31 ± 3**	28 ± 1**##§
Tau	18.3 ± 1.2	26.8 ± 2.4**	26.7 ± 2.3**	28.6 ± 1.2**##§

Data are expressed as means ± SD. +dp/dt, peak positive value of time derivative of LV pressure; -dp/dt, peak negative value of time derivative of LV pressure; tau, the time constant of isovolumic relaxation. \*P < 0.05, \*\*P < 0.01 versus the control group; #P < 0.05, ##P < 0.01 versus the fructose group; §P < 0.05, §§P < 0.01 versus the MS-GFP group.

sus 3.73 ± 1.06, P < 0.01) in FFRs compared with the control rats (Figure 1). Collagen volume fraction of rats receiving the *IL-18* gene markedly increased

compared with the MS-GFP group (8.43 ± 2.57 versus 6.78 ± 1.68, P < 0.05). There was no difference between FFRs and MS-GFP rats.

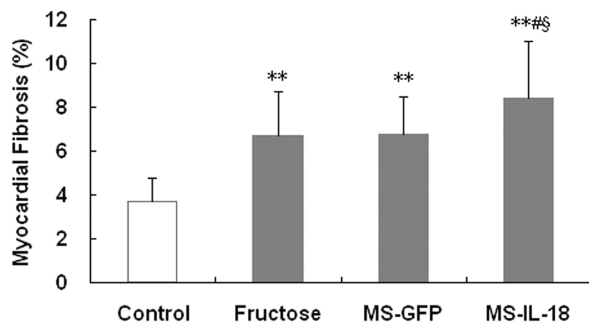
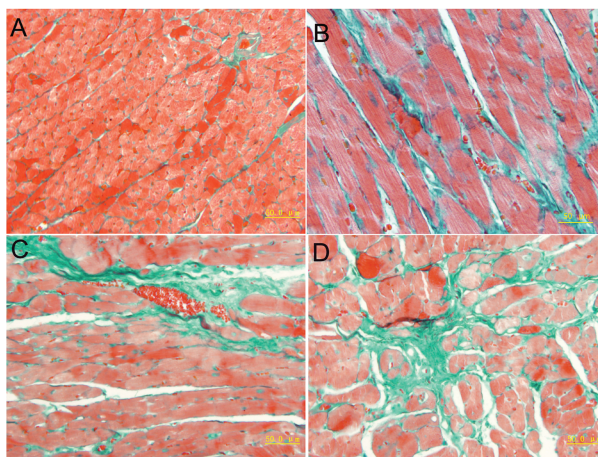


**Figure 1.** Histological examination of the myocardium in experimental rats. Collagen volume fraction of the left ventricle in four groups is shown. Top shows representative microscopic image of the myocardium with Masson's trichrome stain in the control (A), fructose (B), MS-GFP (C) and MS-IL-18 (D) groups (magnification 400×). Lower shows the semi-quantitative evaluation of the collagen volume fraction in four groups of rats. Values are expressed as mean ± SD. \*\*P < 0.01 versus the control group; #P < 0.05 versus the fructose group; §P < 0.05 versus the MS-GFP group. Bar = 50 μm.

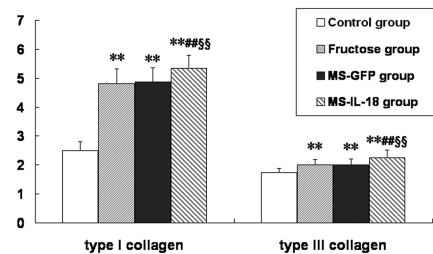


**Figure 2.** Type I and type III collagen mRNA levels in experimental rats. Type I and type III collagen mRNA levels in the control, fructose, MS-GFP and MS-IL-18 groups are shown. \*\*P < 0.01 versus the control group; ##P < 0.01 versus the fructose group; §§P < 0.01 versus the MS-GFP group.

**Expression of Collagen Subtypes**

Both type I and III collagen mRNA levels were increased (4.81 ± 0.52 versus 2.49 ± 0.31, P < 0.01; 2.00 ± 0.20 versus 1.75 ± 0.14, P < 0.01) in FFRs compared with the controls (Figure 2). Overexpression of IL-18 led to the above mRNA levels significantly increased compared with FFR hearts expressing only GFP (5.34 ± 0.46 versus 4.87 ± 0.50, P < 0.01; 2.25 ± 0.26 versus 2.01 ± 0.20, P < 0.01). Figure 3 illustrates immunoreactive fibrillar type I and III collagens protein deposition in LV sections. An increase in type I and III collagen levels were observed in FFRs compared with control rats, and a visible increase in type I and III collagen levels was noted in the MS-IL-18 rats compared with the MS-GFP rats.

**DISCUSSION**

In the present study, we demonstrated that cardiac changes in the MS-like condition of the FFR model are characterized by LV diastolic dysfunction and remarkable collagen accumulation in the cardiac interstitium. Overexpression of IL-18 has significantly aggravated cardiac fibrosis and the diastolic abnormalities but have no effects on systolic parameters. This is somewhat inconsistent with the results of Woldbaek *et al.* (10), which showed daily administration of IL-18 in healthy mice causes LV myocardial systolic and diastolic dysfunction. The explanation for this discrepancy might lie in differences in

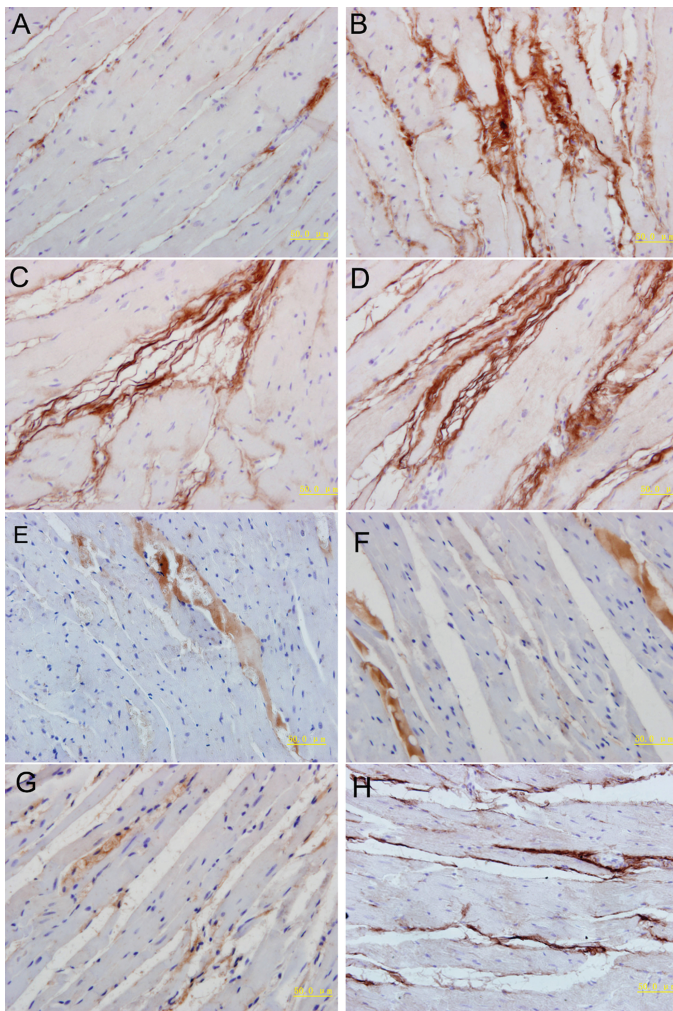


**Figure 3.** Immunohistochemical staining of the myocardium with type I and III collagens in experimental rats. The top two panels show immunohistochemical staining of the myocardium with type I in the control (A), fructose (B), MS-GFP (C) and MS-IL-18 (D) rats (magnification 400 $\times$ ). The lower two panels show immunohistochemical staining of the myocardium with type III in the control (E), fructose (F), MS-GFP (G) and MS-IL-18 (H) rats (magnification 400 $\times$ ). An increase in type I and III collagen levels was observed in FFRs compared with control rats, and visible increases in type I and III collagen levels were noted in the MS-IL-18 rats. Bar = 50  $\mu$ m.

some of the experimental conditions. In Woldbaek's study, 0.5  $\mu$ g mouse IL-18 was injected daily intraperitoneally in healthy male BALB/c mice during a time period of 7 days. However, in our study, FFRs were injected intravenously in the tail with  $1 \times 10^{10}$  plaque-forming units of Ad-IL-18 only once. Our findings suggest a possible mechanism for cardiomyopathy frequently occurred in subjects with MS.

The MS model was achieved by administration of 10% fructose in drinking

water in male Wistar rats during 32 weeks. Our previous studies (11,12) revealed that FFRs showed increased levels of body weight, blood pressure, triglyceride and insulin when compared with the control rats. FFRs developed insulin resistance as assessed by significantly increased homeostasis model assessment in those animals compared with control rats. Insulin resistance appeared to be the common mechanism of fructose-induced diabetes and naturally occurring diabetes

in human subjects. For this particular animal model, we felt that it resembled the human condition in certain key metabolic profiles.

LV diastolic dysfunction can result from two different factors: namely, the alterations in active relaxation, which in turn depends on the biological process of adaptation, and the changes in diastolic compliance, which are direct consequences of chamber diameter and collagen abundance. Ventricular chamber compliance (the pressure-volume curve) depends on the ventricular diameter. Ventricular tissue compliance (the stress-strain curve) is determined by collagen concentration and the degree of fibrosis.

It is generally understood that the pathogenesis of cardiac fibrosis involves the response to two types of stimuli: hormonal and hemodynamic. The former mainly involves the renin-angiotensin-aldosterone system and possibly the endothelin system. Our findings suggest an additional pathway (that is, an inflammatory process) that may interact with the hormonal and hemodynamic stimuli. During the inflammation process that takes place in an overloaded heart (17,18), both macrophages and T cells may release cytokines such as transforming growth factor (TGF)- $\beta$ , and interleukins that can exert an effect on myocardial cells. The metabolism and proliferation of cardiac fibroblasts and cardiomyocytes as well as the extracellular matrix turnover constitute targets for these molecular signals. Collagen I and III first accumulate around intramyocardial coronary arteries, and then the fibrosis extends to the rest of the cardiomyocytes. This process represents the so-called reactive perivascular and interstitial fibrosis. Clearly, understanding the initial reactive events (that is, the activation of perivascular and interstitial fibroblasts) is important. It has been shown that inflammatory cells (17,19) first infiltrate the perivascular domain, where fibroblasts synthesize collagen I mRNA (17) and, subsequently, also infiltrate the interstitial space.

Indeed, chronic subclinical inflammation is part of the MS and may be a causal

factor for certain metabolic abnormalities, such as impaired insulin sensitivity (20). The levels of inflammatory factors such as C-reactive protein (CRP) (21) and IL-18 (4) are elevated in the MS. It appears that IL-18 functions as a pleiotropic proinflammatory cytokine and plays an early role in the inflammatory cascade. IL-18 is able to stimulate the production of tumor necrosis factor- $\alpha$  (5) and secondarily IL-6 (6). In our study, IL-18 expression is altered in infected mice, and this was confirmed by GFP observation of liver sections (12).

Reddy *et al.* (22) showed that IL-18 stimulates fibronectin expression in primary human cardiac fibroblasts via phosphatidylinositol 3-kinase–Akt-dependent NF- $\kappa$ B activation, suggesting that IL-18 *in vivo* may activate signaling pathways leading to cardiac fibrosis. Kim *et al.* (23) reported that IL-18 enhances thrombospondin-1 production in human gastric cancer via the JNK pathway. In addition, the inhibitory effect of heat shock on IL-18 expression is related to the interference of the JNK/AP-1 signaling pathway (24). Recent studies revealed that AP-1 is involved in regulating the expression of IL-18 (25), suggesting that the JNK/AP-1 signaling pathway could have a critical role in mediating the production of IL-18. In the present study, we have shown a direct effect of IL-18 on cardiac fibrosis. After infected adenovirus-mediated transfer of IL-18, the rats did show an increase in collagen volume fraction and expression of type I and III collagen relative to Ad-GFP transgenic rats. Further *in vivo* studies are required to elucidate the precise role of IL-18 in the pathogenesis of myocardial dysfunction. Exploration of the JNK/AP-1 signaling pathway is a valuable future research direction.

In summary, this study suggests an important role of IL-18 in myocardial fibrosis occurring in the MS. It appears that increased IL-18 levels may play an important role in aggravating impaired diastolic function in the MS.

#### ACKNOWLEDGMENTS

This work was supported by a research grant from the National Basic Research

Program of China (973 Program Grant No. 2009CB521904), The Doctoral Fund of Shandong Province (BS2009YY031) and Star Projects of Jinan Young Scientists (09114).

#### DISCLOSURE

The authors declare that they have no competing interests as defined by *Molecular Medicine*, or other interests that might be perceived to influence the results and discussion reported in this paper.

#### REFERENCES

- He J, *et al.* (2001) Risk factors for congestive heart failure in US men and women: NHANES I epidemiologic follow-up study. *Arch. Intern. Med.* 161:996–1002.
- Grandi AM, *et al.* (2006) Metabolic syndrome and morphofunctional characteristics of the left ventricle in clinically hypertensive nondiabetic subjects. *Am. J. Hypertens.* 19:199–205.
- Masugata H, *et al.* (2006) Left ventricular diastolic dysfunction as assessed by echocardiography in metabolic syndrome. *Hypertens. Res.* 29:897–903.
- Hung J, McQuillan BM, Chapman CM, Thompson PL, Beilby JP. (2005) Elevated interleukin-18 levels are associated with the metabolic syndrome independent of obesity and insulin resistance. *Arterioscler. Thromb. Vasc. Biol.* 25:1268–73.
- Puren AJ, Fantuzzi G, Gu Y, Su MS, Dinarello CA. (1998) Interleukin-18 (IFN $\gamma$ -inducing factor) induces IL-8 and IL-1 $\beta$  via TNF $\alpha$  production from non-CD14 human blood mononuclear cells. *J. Clin. Invest.* 101:711–21.
- Olee T, Hashimoto S, Quach J, Lotz M. (1999) IL-18 is produced by articular chondrocytes and induces proinflammatory and catabolic responses. *J. Immunol.* 162:1096–100.
- Brady AJ, Warren JB, Poole-Wilson PA, Williams TJ, Harding SE. (1993) Nitric oxide attenuates cardiac myocyte contraction. *Am. J. Physiol. Heart Circ. Physiol.* 265:H176–82.
- Finkel MS, *et al.* (1992) Negative inotropic effects of cytokines on the heart mediated by nitric oxide. *Science* 257:387–9.
- Kumar A, *et al.* (1996) Tumor necrosis factor alpha and interleukin 1 $\beta$  are responsible for in vitro myocardial cell depression induced by human septic shock serum. *J. Exp. Med.* 183:949–58.
- Woldbaek PR, *et al.* (2005) Daily administration of interleukin-18 causes myocardial dysfunction in healthy mice. *Am. J. Physiol. Heart Circ. Physiol.* 289:H708–14.
- Xing SS, *et al.* (2008) Felodipine reduces cardiac expression of IL-18 and perivascular fibrosis in fructose-fed rats. *Mol. Med.* 14:395–402.
- Tan HW, *et al.* (2010) IL-18 overexpression promotes vascular inflammation and remodeling in a rat model of metabolic syndrome. *Atherosclerosis* 208:350–7.
- Sahn DJ, DeMaria A, Kisslo J, Weyman A. (1978) Recommendations regarding quantitation in M-mode echocardiography: results of a survey of echocardiographic measurements. *Circulation* 58:1072–83.
- Tei C, Nishimura RA, Seward JB, Tajik AJ. (1997) Noninvasive Doppler-derived myocardial performance index: correlation with simultaneous measurements of cardiac catheterization measurements. *J. Am. Soc. Echocardiogr.* 10:169–78.
- Nagueh SF, Middleton KJ, Kopelen HA, Zoghbi WA, Quinones MA. (1997) Doppler tissue imaging: a noninvasive technique for evaluation of left ventricular relaxation and estimation of filling pressures. *J. Am. Coll. Cardiol.* 30:1527–33.
- Masson P. (1992) Trichrome stainings and their preliminary technique. *J. Tech. Methods* 2:75–90.
- Hinglais N, Heudes D, Nicoletti A, Mandet C, Laurent M, Bariéty J, Michel JB. (1994) Co-localization of myocardial fibrosis and inflammatory cells in rats. *Lab. Invest.* 70:286–94.
- Nicoletti A, *et al.* (1995) Left ventricular fibrosis in renovascular hypertensive rats: effect of losartan and spironolactone. *Hypertension* 26:101–11.
- Haller H, *et al.* (1995) Monocyte infiltration and c-fms expression in hearts of spontaneously hypertensive rats. *Hypertension* 25:132–8.
- Esposito K, Giugliano D. (2004) The metabolic syndrome and inflammation: association or causation? *Nutr. Metab. Cardiovasc. Dis.* 14:228–32.
- Florez H, *et al.* (2006) C-reactive protein is elevated in obese patients with the metabolic syndrome. *Diabetes Res. Clin. Pract.* 71:92–100.
- Reddy VS, *et al.* (2008) Interleukin-18 stimulates fibronectin expression in primary human cardiac fibroblasts via PI3K–Akt-dependent NF- $\kappa$ B activation. *J. Cell Physiol.* 215:697–707.
- Kim J, *et al.* (2006) IL-18 enhances thrombospondin-1 production in human gastric cancer via JNK pathway. *Biochemical and Biophysical Research Communications* 344:1284–9.
- Wang Y, Li C, Wang X, Zhang J, Chang Z. (2002) Heat shock response inhibits IL-18 expression through the JNK pathway in murine peritoneal macrophages. *Biochemical and Biophysical Research Communications* 296:742–8.
- Kim YM, Im JY, Han SH, Kang HS, Choi I. (2000) IFN- $\gamma$  up-regulates IL-18 gene expression via IFN consensus sequence-binding protein and activator protein-1 elements in macrophages. *J. Immunol.* 165:3198–205.